

## Simplified Analysis of Electron-Hole Recombination in Zn- and O-Doped GaP

C. H. Henry, R. Z. Bachrach, and N. E. Schumaker

*Bell Laboratories, Murray Hill, New Jersey 07974*

(Received 12 April 1973)

An analysis of the recombination kinetics of three differently annealed GaP samples of a crystal doped with Zn and O is presented. The kinetics are described in terms of four parameters: a hole recombination lifetime  $T_1$ ; an emission rate  $e_1$  for electrons to be thermally excited from the Zn-O center back into the conduction band; a shunt-path lifetime  $T_{SH}$ ; and a rate  $c_1$  for capture of electrons by the Zn-O centers. Rate  $e_1$  had been previously determined by Jayson, Bachrach, Dapkus, and Schumaker. Two other parameters  $T_1$  and  $(T_{SH}^{-1} + c_1)$  were directly measured.  $T_{SH}$  and  $c_1$  were separately determined by evaluating the ratio  $T_{SH}^{-1}/(T_{SH}^{-1} + c_1)$ , which is the fraction of the carriers leaving the conduction band through the shunt path. This ratio was deduced in two independent ways from analysis of the time dependence of the red and green luminescence. In the most efficient sample, the parameters at 298 K were  $e_1^{-1} = 220 \pm 10$  nsec,  $T_1 = 630 \pm 30$  nsec,  $T_{SH} = 60 \pm 10$  nsec, and  $c_1^{-1} = 10 \pm 1$  nsec. About  $0.60 \pm 0.05$  of the recombination in this sample was through the Zn-O centers. The measured radiative efficiency was  $0.29 \pm 0.03$ , indicating that about half the recombination was radiative. The radiative and nonradiative hole recombination times were  $(T_1)_{rad} = 1310 \pm 130$  nsec and  $(T_1)_{nonrad} = 1210 \pm 90$  nsec for this sample with  $p \approx 2 \times 10^{17}/\text{cm}^3$  ( $N_A - N_D = 2.5 \times 10^{17}/\text{cm}^3$ ). These lifetimes are in good agreement with those deduced previously by Jayson, Bhargava, and Dixon. The effect of annealing is to change  $T_{SH}$  from about 5 to 60 nsec and to increase the Zn-O center concentration by 5 or 6 times. These changes increased the recombination through the Zn-O center by a factor of  $25 \pm 5$ . Annealing also appeared to decrease the majority carrier concentration by about 10%.

### I. INTRODUCTION

Nonradiative recombination is one of the few subjects in semiconductor physics that is still poorly understood. It is quite likely that the primary source of nonradiative recombination is recombination through deep traps. The nature of such traps and the detailed physical mechanisms whereby the nonradiative transitions take place have not yet been identified. Recently a variety of junction-capacitance and junction-current measurements have been developed by Sah and others which detect deep traps in semiconductors.<sup>1</sup> These techniques have been intensively applied to Zn- and O-doped GaP by Bjorklund and Grimmeiss,<sup>2</sup> Kukimoto *et al.*,<sup>3</sup> Henry *et al.*,<sup>4</sup> and Lang.<sup>5</sup> These measurements have revealed only two traps that exist in large concentrations, the Zn-O center and the deep O donor. Luminescence studies by Jayson *et al.*<sup>6</sup> have shown that the Zn-O center is an efficient recombination center which can have internal luminescence efficiencies as high as 17%. Luminescence studies of the O donor by Jayson *et al.*<sup>6</sup> have also indicated that this center is important in recombination. However, two recent detailed capacitance studies by Henry *et al.*<sup>4</sup> and Lang<sup>5</sup> have shown that the recombination through the O donor is no more than a few percent of the recombination through the Zn-O center and therefore that this recombination path can be neglected. It may be that the residual recombination is due to other traps present in much smaller concentrations than the Zn-O center. Recently, Smith<sup>7</sup> has revealed a

variety of traps in GaP, present in small concentrations, by measurement of thermally stimulated junction currents. The importance of these traps in electron-hole recombination was not evaluated. This paper is part of a continuing study of nonradiative recombination in GaP. It is an attempt to learn precisely what fraction of the minority carriers recombine through the Zn-O center, how much of this recombination is radiative, and what is the contribution of other paths of recombination (the shunt path) to the minority carrier lifetime. These results determine the extent that other traps, as yet undetected, are contributing to electron-hole recombination in Zn- and O-doped GaP.

The kinetics of electron-hole recombination in Zn- and O-doped GaP has been under intensive study since the paper by van der Does de Bye in 1966.<sup>8</sup> Many papers have been written<sup>6,9-13</sup> on this subject since then, but the majority of these are mathematically complex and utilize a large number of parameters. In this paper, we analyze the recombination in a simple and accurate way that uses as few parameters and makes as few assumptions as possible. The first complete treatment of the room-temperature recombination kinetics of this center was given by Jayson, Bhargava and Dixon.<sup>9</sup> The model that we use is the same as they and others<sup>6,12,13</sup> since have used, but we start from the following simplifications.

First, because the hole bound to the Zn-O center is in thermal equilibrium with the holes in the valence band, as shown by Jayson and Bachrach,<sup>14</sup> no equation has to be solved for the bound-hole

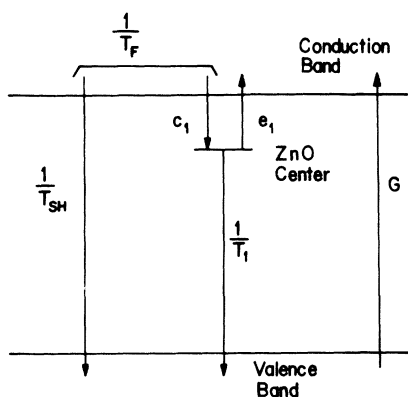


FIG. 1. Schematic diagram showing the shunt path, capture onto the Zn-O level, thermal emission and recombination from the Zn-O level, and generation of carriers.

concentration. Since the holes are in thermal equilibrium, all electron-hole recombination processes involving the electron bond to the Zn-O center contribute to a single rate which we will call  $1/T_1$  (see Fig. 1).

Second, no attempt is made to subdivide  $1/T_1$  into radiative and nonradiative (Auger) components. This division is made later by comparing the fraction of the recombination through the Zn-O center with the measured internal radiative efficiency.

Third, the recombination through the deep O donor is not explicitly treated. This and other recombination mechanisms, apart from the Zn-O center, are considered to contribute to a shunt path of recombination in parallel with the Zn-O center and thus do not have to be considered explicitly. Studies of the time dependence of the minority-carrier concentration in Sec. III C show that the Zn-O center is the only significant trap that slowly reemits electrons to the conduction band after capture at room temperature. Therefore reemission from the shunt-path traps is not considered and this path may be characterized by a single capture rate  $1/T_{SH}$ .

The complete recombination kinetics are fixed by four parameters, as shown in Fig. 1. The two parameters not yet mentioned are the capture rate for electrons onto the Zn-O centers,  $c_1$ , and the rate of thermal emission of electrons back into the conduction band,  $e_1$ . The object of our study is to establish these four parameters in a straightforward and accurate manner. Several of these parameters are readily determined.

The thermal-emission rate  $e_1$  versus temperature can be determined from the decay rate of the red luminescence in a sample in which the Zn-O concentration and the hole concentration are both quite low. In such a sample, the bound electron decays

by thermal emission back into the conduction band and multiple capture effects are negligible. Using such a sample, the thermal-emission rate was measured by Jayson *et al.*<sup>8</sup> who found  $e_1^{-1}$  to be 220 nsec at 298 K. We will make use of their data, since  $e_1$  should not depend upon the sample.

The hole recombination rate  $1/T_1$  is also readily determined since at low temperature  $e_1$  is negligible. The red luminescence decays with rate  $1/T_1$ , which varies slowly with temperature in the 200–400 K temperature range. We can determine  $1/T_1$  over this range from an extrapolation of the low-temperature decay rate of the red luminescence, as shown in Fig. 2. This extrapolation is an important simplification and is a major difference between this treatment and the earlier work.<sup>11</sup>

One other parameter can be evaluated in a straightforward manner. The sum of the capture rates,

$$\frac{1}{T_F} = c_1 + \frac{1}{T_{SH}}, \quad (1)$$

is approximately equal to the time constant for the rapid rise and fall of the minority-carrier concentration. We call  $T_F$  the fast minority-carrier lifetime. We can accurately measure  $T_F$  from the

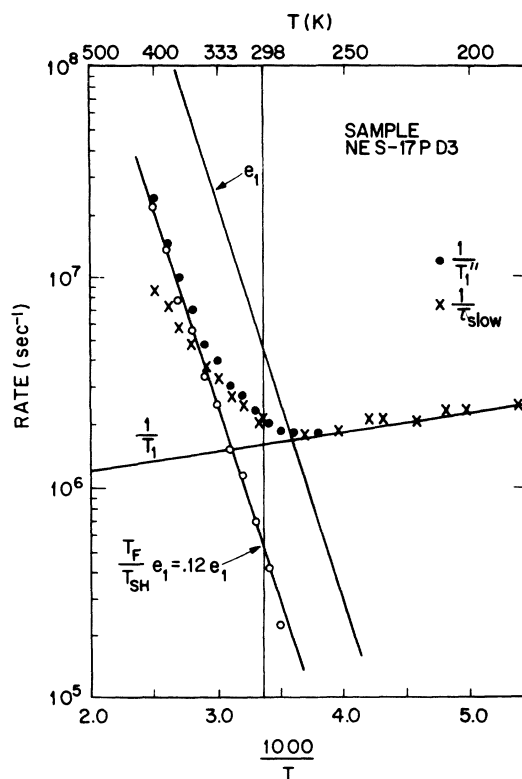


FIG. 2. Measured red-luminescence decay rate (points labeled x),  $1/T_1'$  (solid dots),  $(T_F/T_{SH})e_1$  (open circles),  $e_1$  (solid curve), and  $1/T_1$  (solid curve).

fast rise (or fall) of the green luminescence at room temperature, as shown by Bachrach and Lormor.<sup>15</sup> This is illustrated in Fig. 3.

The kinetics of recombination are completely established by one final parameter,  $T_F/T_{SH}$ , which represents the fraction of minority carriers which initially leave the conduction band through the shunt path (see Fig. 1). This parameter is crucial in determining how much recombination takes place through the Zn-O center as was discussed previously by Jayson *et al.*<sup>11</sup> We will determine this parameter in two independent ways: first, by analyzing the red-luminescence decay rate versus temperature, and second, by studying the relative magnitudes of the rapid and slow increases of the green luminescence in response to a long pulse of excitation.

Using these values of  $T_F/T_{SH}$ , we calculate the fraction of the recombination through the Zn-O center,  $F$ . By comparing the measured internal radiative efficiency  $\eta$  with  $F$ , we are able to learn what fraction of the recombination through the Zn-O center is radiative and thereby we can determine the radiative and nonradiative (Auger) decay rates.

All experiments are carried out on three samples obtained from the same Zn- and O-doped epitaxial layer, but annealed in different ways as shown in Table I. The layers were 20- $\mu$  thick and had a net acceptor concentration of  $2.5 \times 10^{17} \text{ cm}^{-3}$ . Capacitive analysis showed the substitutional-oxygen concentration was about  $(2-3) \times 10^{18} \text{ cm}^{-3}$ . High-efficiency  $p$  layers such as this were grown in a ground-glass sealed-quartz vessel from 1020 to 980° C. From analysis of this series of samples, we are able to ascertain how the relative ZnO concentration and the shunt-path recombination rate change during annealing and how much recombination takes place through the Zn-O center in an efficient sample.

In Sec. II we present the theory of the recombination kinetics. The kinetic parameters are deter-

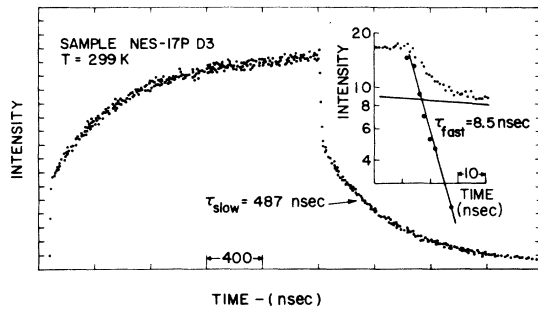


FIG. 3. Rise and fall of the green luminescence at 5500 Å versus time at room temperature. The insert shows an expanded view of the fast decay from which  $\tau_{fast}$  was measured.

mined from direct measurements in Sec. III A, from the decay rate of the red luminescence in Sec. III B, and from the time dependence of the green luminescence in Sec. III C. Internal efficiency measurements are reported in Sec. IV. Our results are summarized in Sec. V and Tables I, II, and III.

## II. KINETIC EQUATIONS

The rate equations for the minority-carrier concentration  $n$  and the bound-electron concentration  $n_1$  may be readily written down with the aid of Fig. 1 as

$$\dot{n} + \frac{1}{T_F} n = G + e_1 n_1, \quad (2)$$

$$\dot{n}_1 + \left( \frac{1}{T_1} + e_1 \right) n_1 = c_1 n. \quad (3)$$

These equations neglect saturation of the Zn-O center.

Any transient solution of these equations will in general involve two exponentials in time. The two rates will be the solution of the secular equation

$$\lambda^2 - \left( \frac{1}{T_F} + \frac{1}{T_1'} \right) \lambda + \frac{1}{T_F} \frac{1}{T_1''} = 0, \quad (4)$$

where

$$\frac{1}{T_1'} = \frac{1}{T_1} + e_1 \quad (5)$$

and

$$\frac{1}{T_1''} = \frac{1}{T_1} + e_1 \frac{T_F}{T_{SH}}. \quad (6)$$

We have made use of Eq. (1) in deriving Eq. (6).

The two solutions of Eq. (4) give the two rates  $\lambda = 1/\tau_{fast}$  and  $\lambda = 1/\tau_{slow}$ :

$$\left. \begin{array}{l} \frac{1}{\tau_{fast}} \\ \frac{1}{\tau_{slow}} \end{array} \right\} = \frac{1}{2} \left( \frac{1}{T_F} + \frac{1}{T_1'} \right) \pm \left[ \frac{1}{4} \left( \frac{1}{T_F} + \frac{1}{T_1'} \right)^2 - \frac{1}{T_F} \frac{1}{T_1''} \right]^{1/2}. \quad (7)$$

In the limit that  $1/T_F \gg 1/T_1$ ,  $e_1$ , which is a good approximation at room temperature and lower, Eq. (7) can be found to reduce to

$$\frac{1}{\tau_{fast}} \cong \frac{1}{T_F}, \quad (8)$$

$$\frac{1}{\tau_{slow}} \cong \frac{1}{T_1''} = \frac{1}{T_1} + e_1 \frac{T_F}{T_{SH}}. \quad (9)$$

In this limit, the bound-state density builds up and decays with rate  $1/T_1''$ . In response to a pulse of excitation  $G$ , in this approximation, the minority-carrier concentration rises with time constant  $T_F$  to  $GT_F$ , as the carriers are initially trapped on the Zn-O center, and then rises with time constant  $T_1''$  to the steady-state value. In the absence of suc-

TABLE I. Directly measured parameters.

Sample	Annealing procedure	$e_1^{-1}$ (nsec)	$T_F$ (nsec)	$T_1$ (nsec)	$\eta$
NES 17P UA	None	220 ± 10	4.6 ± 1.0	540 ± 40	0.014 ± 0.001
NES 17P C3	10 h at 600 °C	220 ± 10	6.2 ± 1.0	630 ± 30	0.18 ± 0.02
	10 h at 600 °C				
NES 17P D3	10 h at 500 °C	220 ± 10	8.5 ± 0.5	630 ± 30	0.29 ± 0.03

cessive capture of minority carriers by the Zn-O centers, the lifetime of a bound electron on the Zn-O center would be  $T_1'$ , given by (5). The result of multiple capture is effectively to decrease the net rate of thermal emission from  $e_1$  to  $(T_F/T_{SH}) \times e_1$  and to change the lifetime of a bound electron from  $T_1'$  to  $T_1''$ . This can be shown by substituting the approximate solution of Eq. (2)  $n \approx (G + e_1 n_1) T_F$ , into Eq. (3).

The steady-state solutions of Eqs. (2) and (3) are

$$n_1 = G \left( 1 - \frac{T_F}{T_{SH}} \right) T_1'' \quad (10)$$

and

$$n = G T_s, \quad (11)$$

where

$$\frac{1}{T_s} = \frac{1}{T_{SH}} + \frac{c_1}{1 + e_1 T_1}. \quad (12)$$

We will refer to  $T_s$  as the steady-state minority-carrier lifetime. This lifetime is longer than  $T_F$  because thermal reemission of electrons from ZnO has reduced  $c_1$  in the steady state to a net capture rate  $c_1/(1 + e_1 T_1)$ . The formula for the net capture rate can be derived using the steady-state solutions of Eqs. (2) and (3).

### III. DETERMINATION OF THE KINETIC PARAMETERS

#### A. Directly Measured Parameters

Three of the four kinetic parameters  $e_1$ ,  $T_1$ , and  $T_F$  are readily measured. Their measurement has already been discussed in Sec. I. These parameters are listed in Table I for the three samples measured in this paper. The samples are from the same epitaxial layer, which was quenched to room temperature after growth. Two of the samples then underwent annealing treatments that are specified in the table.

The three samples differ greatly in radiative efficiency, yet the three parameters listed in Table I are very similar. The differences between the three samples are primarily reflected in the fourth kinetic parameter,  $T_F/T_{SH}$ , which is determined by

two different methods in Secs. IIIB and IIIC.

#### B. Analysis of the Decay Rate of the Red Luminescence

The red luminescence decays with rate  $\tau_{slow}^{-1}$ . By measuring  $\tau_{slow}$  as a function of temperature we are able to determine  $T_1''$  and thereby  $T_F/T_{SH}$ . The relation between  $T_1''$  and  $\tau_{slow}$  is given by Eq. (4) with  $\lambda = 1/\tau_{slow}$ :

$$\frac{1}{T_1''} = \frac{1}{\tau_{slow}} \left[ 1 + T_F \left( \frac{1}{T_1'} - \frac{1}{\tau_{slow}} \right) \right]. \quad (13)$$

The measured rate  $\tau_{slow}^{-1}$  for the most efficient sample is shown in Fig. 2. At low temperature,  $\tau_{slow} = T_1$ .  $T_1$  was determined as a function of temperature by a linear extrapolation of the low-temperature data, as shown in Fig. 2.  $1/T_1'$  was found from the sum of  $1/T_1$  and  $e_1$  (also shown in Fig. 2).  $T_F$  was measured at room temperature from the fast rise of the green luminescence.  $T_F$  was assumed to be independent of temperature. With these parameters fixed,  $T_1''^{-1}$  was then calculated.  $1/T_1''$  is plotted as solid dots in Fig. 2. Below room temperature  $1/T_1''$  is approximately equal to  $1/\tau_{slow}$ , whereas at 400 K,  $1/T_1''$  is almost three times as great as  $1/\tau_{slow}$ . Subtracting  $1/T_1$  from  $1/T_1''$  leaves  $(T_F/T_{SH})e_1$ . These data, shown by the open circles in Fig. 2, have almost the same slope as  $e_1$ . From these data we deduce that  $T_F/T_{SH}$  is roughly constant and equal to  $0.12 \pm 0.02$  for this sample.

The fraction of recombination  $F$  that takes place through the Zn-O center is given by dividing the recombination rate for bound carriers,  $n_1/T_1$ , by the carrier generation rate  $G$ .

$$F = \frac{n_1}{T_1 G}. \quad (14)$$

$F$  can also be derived by dividing the net rate of capture of carriers onto the Zn-O center,  $c_1 n / (1 + e_1 T_1)$ , by the carrier generation rate  $G$ :

$$F = \frac{c_1 n}{(1 + e_1 T_1) G}. \quad (15)$$

We will use this equation to evaluate  $F$  in Sec. IIIC.

Substituting the steady-state value of  $n_1$ , given by Eq. (10), into Eq. (14), we find

$$F = \frac{(1 - T_F/T_{SH})T_1''}{T_1}. \quad (16)$$

The values of  $F$  for the two annealed samples are listed in Table II. For the unannealed sample analysis of  $1/T_1''$  versus temperature showed that  $T_F/T_{SH}$  was slightly less than unity, but  $1 - T_F/T_{SH}$  could not be evaluated accurately. Thus, no value of  $F$  is listed in Table II for this sample.

### C. Analysis of the Time Dependence of the Green Luminescence at 5500 Å

The fourth kinetic parameter  $T_F/T_{SH}$  can be ascertained from the time dependence of the green luminescence. The green luminescence is proportional to the minority-carrier concentration. In response to a long pulse of excitation  $G$ , the minority-carrier concentration rises to approximately  $GT_F$  and then to the steady-state value  $GT_s$ , as shown in Fig. 3. From analysis of this data  $T_s/T_F$  can be determined. Combining Eqs. (1) and (12) we find that

$$c_1 T_F = 1 - \frac{T_F}{T_{SH}} = \left(1 - \frac{T_F}{T_s}\right) \left(\frac{1 + e_1 T_i}{e_1 T_1}\right). \quad (17)$$

From this equation  $T_F/T_{SH}$  may be calculated. The fraction of recombination through the Zn-O center is given by Eq. (15). Evaluating  $n$  in this equation with Eq. (11) and using Eqs. (12) and (17), we find

$$F = \left(\frac{1 - T_F/T_s}{e_1 T_1}\right). \quad (18)$$

$T_s/T_F$  is approximately given by the ratio of the steady-state amplitude and the initial fast-rising amplitude of the green luminescence. Accurate determination of  $T_s/T_F$  requires a more accurate analysis of the time dependence of the minority-carrier concentration. In response to a long pulse of excitation  $G$ , the minority-carrier concentration increases from zero to the steady-state value  $GT_s$  as

$$n(t) = A(1 - e^{-t/\tau_{fast}}) + (GT_s - A)(1 - e^{-t/\tau_{slow}}). \quad (19)$$

Constant  $A$  is set by the initial condition imposed

by Eq. (2) that

$$\dot{n}(0) = G = \frac{A}{\tau_{fast}} + \frac{GT_s - A}{\tau_{slow}}. \quad (20)$$

The solution of this equation is

$$A = \frac{G\tau_{fast}(1 - T_s/\tau_{slow})}{(1 - \tau_{fast}/\tau_{slow})}. \quad (21)$$

The ratio of the steady-state minority-carrier concentration  $n_s$  to the fast-rising minority-carrier concentration  $n_i$  is

$$\frac{n_s}{n_i} = \frac{GT_s}{A} = \frac{T_s}{\tau_{fast}} \frac{(1 - \tau_{fast}/\tau_{slow})}{(1 - T_s/\tau_{slow})}. \quad (22)$$

The carrier concentrations will drop from the bulk value to zero at the surfaces of the epitaxial layer owing to surface recombination. The green-luminescence intensity is proportional to the average value of the minority-carrier concentration  $\langle n \rangle$ . This value will be reduced from the bulk value by surface recombination according to

$$\langle n \rangle \approx n_{bulk}(1 - 2L/t), \quad (23)$$

where  $L$  is the diffusion length and  $t$  is the thickness of the layer, which is  $20 \mu$  in these experiments.  $L$  is given by  $(D\tau_{fast})^{1/2}$  for  $n_i$  and by  $(DT_s)^{1/2}$  for  $n_s$ . Combining Eqs. (22) and (23), we have

$$\begin{aligned} \frac{\langle n_s \rangle}{\langle n_i \rangle} &= \frac{\tau_s}{\tau_{fast}} \frac{(1 - \tau_{fast}/\tau_{slow})}{(1 - \tau_s/\tau_{slow})} \\ &\times \frac{[1 - 2(DT_s)^{1/2}/t]}{[1 - 2(D\tau_{fast})^{1/2}/t]} \end{aligned} \quad (24)$$

We estimate  $D = 2 \text{ cm}^2/\text{sec}$ , which corresponds to a mobility of 80 at room temperature. Consider the most efficient sample. At room temperature  $\tau_{fast} \approx T_F$ . An exact relation between these two quantities is given by Eq. (7), which can be approximated in the limit of  $\tau_{fast} \approx T_F$  as

$$\tau_{fast} \approx \frac{T_F}{1 + \tau_{fast}(1/T_1' - 1/T_1'')} \quad (25)$$

For this sample  $\tau_{fast} = 8.5 \text{ nsec}$ ,  $T_1' = 174 \text{ nsec}$ , and  $T_1'' = 487 \text{ nsec}$ . Then Eq. (25) gives  $T_F = 1.03\tau_{fast}$ . We use this relation to evaluate the

TABLE II. Properties deduced from analysis of the red luminescence.

Sample	$T_1''$ (nsec)	$T_F/T_{SH}$	$F$	$\eta/F$	$T_{SH}$ (nsec)	$c_1^{-1}$ (nsec)
NES 17P UA	171 ± 8	≈ 1.0	...	...	≥ 4.6	...
NES 17P C3	435 ± 25	0.15 ± 0.03	0.59 ± 0.04	0.31 ± 0.04	45 ± 10	8.0 ± 1.3
NES 17P D3	465 ± 22	0.12 ± 0.02	0.65 ± 0.05	0.45 ± 0.06	71 ± 13	9.7 ± 0.6

first term in Eq. (24). The data in Fig. 3 show  $\langle n_s \rangle / \langle n_i \rangle = 2.50 \pm 0.12$ . The other correction factors in Eq. (24) are evaluated with the approximations  $T_s / \tau_{\text{fast}} = 2.5$  and  $\tau_{\text{slow}} = T_1'$ . Then Eq. (24) reduces to

$$\frac{\langle n_s \rangle}{\langle n_i \rangle} = \frac{T_s}{T_F} (1.03) \frac{(0.982)}{(0.956)} \frac{(0.794)}{(0.869)}$$

$$= 0.97 T_s / T_F = 2.50 \pm 0.12$$

or

$$T_s / T_F = 2.58 \pm 0.12.$$

The corrections for  $A$  not equal to  $GT_F$  and for the effect of surface recombination tend to cancel each other. As a result  $T_s / T_F$  is almost equal to the ratio of the steady-state and initial amplitudes of the green luminescence. The values of  $T_{\text{SH}}$ ,  $F$ , and  $T_s$  and the steady-state diffusion length

$$L_s = (DT_s)^{1/2} \quad (26)$$

are tabulated in Table II for the three samples. The ratio of the concentration of the Zn-O center after annealing to the concentration before annealing,  $N/N_{\text{UA}}$ , is found from the ratio of the measured capture rates,  $c_1$ . This ratio is also included in the Table III.

#### IV. MEASUREMENT OF INTERNAL RADIATIVE EFFICIENCIES

The internal radiative efficiencies of the three samples were measured by a substitution technique utilizing an integrating sphere and a reference-light-emitting diode which has been calibrated with respect to a standard lamp.<sup>16</sup> Detection was through a spectrometer at 1.86 eV, thus eliminating the need to correct for the infrared spectral component. Efficiencies were measured before and after epoxy encapsulation to determine the optical coupling efficiency.<sup>17</sup> Excitation was provided by the 4880-Å argon-ion-laser line, which has a penetration depth  $1/\alpha$  of 10.3  $\mu$  at 300 K. The excitation was kept low enough so that the centers were unsaturated.

The highest efficiency was measured in NES 17P D3. The efficiency measured in air was 6.4% and the increase on encapsulation was 1.88

to 12.1%. This converts to an optical-coupling efficiency of 0.53 and therefore the internal efficiency is  $(22.9 \pm 1.5)\%$ . The measured efficiencies were corrected for losses due to surface recombination by multiplying the measured efficiencies by  $(1 - L_s \alpha)^{-1}$ , where  $L_s$  is the diffusion length given in Table III and  $\alpha$  is the absorption coefficient of the laser. This correction increased the internal radiative efficiency of sample NES 17P D3 to  $(29 \pm 3)\%$ . The bulk radiative efficiencies of the three samples are listed in Table I. The fraction of the recombination through the Zn-O center that is radiative is  $\eta/F$ . This fraction is given in Tables II and III for the corresponding values of  $F$ . The average value of  $\eta/F$  for the most efficient sample was  $0.48 \pm 0.04$ . The radiative and non-radiative lifetimes are given by

$$(T_1^{-1})_{\text{rad}} = (\eta/F) T_1^{-1}, \quad (27)$$

$$(T_1^{-1})_{\text{nonrad}} = (1 - \eta/F) T_1^{-1}. \quad (28)$$

For the most efficient sample, these lifetimes are  $(T_1)_{\text{rad}} = 1310 \pm 130$  nsec and  $(T_1)_{\text{nonrad}} = 1210 \pm 90$  nsec. The sample had a minority-carrier concentration of  $p = 2 \times 10^{17}$  cm<sup>-3</sup>, which was deduced from a capacitance profile that gave  $N_A - N_D = 2.5 \times 10^{17}$  cm<sup>-3</sup>.

These results are in remarkably good agreement with those of Jayson, Bhargava, and Dixon.<sup>11</sup> According to Eq. (8) of their paper, for a carrier concentration of  $p = 2 \times 10^{17}$  cm<sup>-3</sup>,  $(T_1)_{\text{rad}} = 1720$  nsec and  $(T_1)_{\text{nonrad}} = 1050$  nsec.

#### V. SUMMARY AND DISCUSSION

The parameters that describe kinetics of recombination are listed in Tables I, II, and III. Parameters such as  $T_F$  which could be measured in a direct manner are listed in Table I. The remaining parameters such as  $T_{\text{SH}}$  and  $F$  were established in two independent ways by analyzing the time dependence of the red and green luminescence. These parameters are listed in Tables II and III. In general there was good agreement between these two methods. Averaging the results of Tables II and III, we find that about 60% of the recombination was through the Zn-O center in the most efficient sample. About 48% of this recombination was radiative, resulting in an internal radiative efficiency of 29%. The most efficient sample had a

TABLE III. Properties deduced from analysis of the green luminescence.

Sample	$\frac{T_s}{T_F}$	$T_s$ (nsec)	$L_s$ ( $\mu$ )	$T_F/T_{\text{SH}}$	$F$	$\eta/F$	$T_{\text{SH}}$ (nsec)	$c_1^{-1}$ (nsec)	$N/N_{\text{UA}}$
NES 17P UA	$1.06 \pm 0.01$	$4.9 \pm 1.0$	$0.99 \pm 0.10$	$0.92 \pm 0.01$	$0.024 \pm 0.005$	$0.60 \pm 0.13$	$4.9 \pm 1.0$	$56 \pm 14$	1.0
NES 17P C3	$2.06 \pm 0.10$	$12.8 \pm 2.0$	$1.6 \pm 0.12$	$0.31 \pm 0.03$	$0.37 \pm 0.05$	$0.49 \pm 0.08$	$30 \pm 5$	$9.0 \pm 1.0$	$6.2 \pm 1.5$
NES 17P D3	$2.58 \pm 0.12$	$21.9 \pm 1.6$	$2.09 \pm 0.08$	$0.17 \pm 0.03$	$0.55 \pm 0.06$	$0.52 \pm 0.08$	$50 \pm 9$	$10.2 \pm 1.0$	$5.5 \pm 1.5$

shunt-path lifetime of about 60 nsec and a capture rate onto the Zn-O center of about  $1/(10 \text{ nsec})$ . In contrast to this sample, the unannealed sample had a shunt-path lifetime of about 5 nsec and a capture rate of about  $1/(56 \text{ nsec})$ . Thus annealing not only increased the Zn-O center concentration five or sixfold, but it decreased the shunt-path recombina-

tion rate by an order of magnitude. These two effects increased the efficiency of the annealed sample about 25 times over the efficiency of the unannealed sample. Increases in efficiency of this magnitude were observed by Toyama and Kasami,<sup>18</sup> who attributed them solely to changes in the Zn-O complex concentration.

---

<sup>1</sup>C. T. Sah, L. Forbes, L. I. Rosier, and A. F. Tosch, Jr., *Solid-State Electron.* **13**, 759 (1970).

<sup>2</sup>G. Bjorklund and H. G. Grimmeiss, *Solid-State Electron.* **14**, 589 (1971).

<sup>3</sup>H. Kukimoto, C. H. Henry, and F. R. Merritt, *Phys. Rev. B* **7**, 2486 (1973).

<sup>4</sup>C. H. Henry, H. Kukimoto, G. L. Miller, and F. R. Merritt, *Phys. Rev. B* **7**, 2499 (1973).

<sup>5</sup>D. V. Lang, *Bull. Am. Phys. Soc.* **18**, 381 (1973).

<sup>6</sup>J. S. Jayson, R. Z. Bachrach, P. D. Dapkus, and N. E. Schumaker, *Phys. Rev. B* **6**, 2357 (1972).

<sup>7</sup>B. L. Smith, *Appl. Phys. Lett.* **21**, 350 (1972).

<sup>8</sup>J. A. W. van der Does de Bye, *Phys. Rev.* **147**, 589 (1966).

<sup>9</sup>W. Rosenzweig, W. H. Hackett, Jr., and J. S. Jayson, *J. Appl. Phys.* **40**, 4477 (1969).

<sup>10</sup>A. Kasami, *Jap. J. Appl. Phys.* **9**, 946 (1970).

<sup>11</sup>J. S. Jayson, R. N. Bhargava, and R. W. Dixon, *J. Appl. Phys.* **41**, 4972 (1970).

<sup>12</sup>J. M. Dishman, M. DiDomenico, and R. Caruso, *Phys. Rev. B* **2**, 1988 (1970).

<sup>13</sup>W. H. Hackett, Jr., R. H. Saul, R. W. Dixon, and G. W. Kammlott, *J. Appl. Phys.* **43**, 2857 (1972).

<sup>14</sup>J. S. Jayson and R. Z. Bachrach, *Phys. Rev. B* **4**, 477 (1971).

<sup>15</sup>R. Z. Bachrach and O. G. Lorimor, *J. Appl. Phys.* **43**, 500 (1972).

<sup>16</sup>J. M. Ralston and R. Z. Bachrach (unpublished).

<sup>17</sup>W. B. Joyce, R. Z. Bachrach, R. W. Dixon, and D. A. Sealer (unpublished).

<sup>18</sup>M. Toyama and A. Kasami, *Jap. J. Appl. Phys.* **11**, 860 (1972).